

**MINERALOGY AND COOLING HISTORY OF UNGROUPED ACHONDRITE ERG CHECH 002.** T. Mikouchi<sup>1</sup> and M. E. Zolensky<sup>2</sup>, <sup>1</sup>The University Museum, The University of Tokyo, Hongo, Tokyo 113-0033, Japan (mikouchi@um.u-tokyo.ac.jp), <sup>2</sup>ARES, NASA Johnson Space Center, Houston, TX 77058, USA.

**Introduction:** Recent recovery of tons of meteorites from northwestern Africa has yielded unusual meteorites that have not been found so far. Erg Chech 002 (EC002) is one of such meteorites discovered in Algeria in 2020 [1]. Its oxygen isotope composition ( $\Delta^{17}\text{O}$ ) is located intermediate between the fields of eucrites and angrites, and close to anomalous eucrites Bunburra Rockhole, Emmaville, Asuka-881394 and EET 92023, but EC002 is distinct in mineralogy and petrology, resulting in its classification as an ungrouped achondrite [1]. Besides well-established achondrite groups such as HED meteorites, angrites and aubrites, we now have achondritic samples showing evidence for high grade metamorphic and igneous processes directly related to precursors of many carbonaceous and ordinary chondrite groups [e.g., 2]. Therefore, it is important to document new ungrouped achondrite samples to better understand diversity of igneous processes occurred in the differentiated bodies in the early solar system.

**Sample and Methods:** A polished thin section (PTS) of EC002 was made from a 6.2 g slice to include the largest megacryst (Fig. 1). The PTS was observed by optical microscope and mineral compositions were obtained by electron microprobes JEOL JXA 8900L and JXA 8530F. Phase identification of feldspar and silica minerals was performed by JASCO NRS-1000 micro Raman spectrometer.

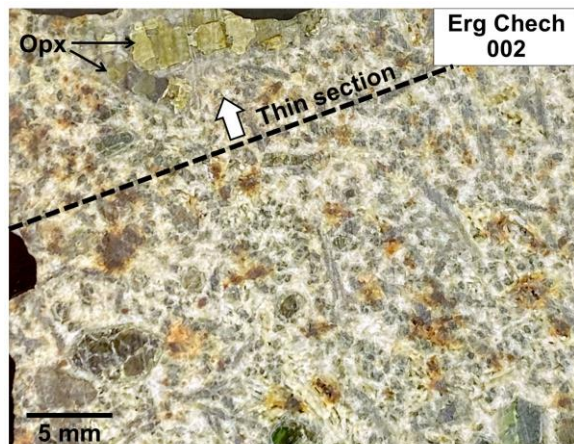


Fig. 1 Optical photomicrograph of the EC002 slice used for this study. Opx: orthopyroxene megacrysts.

**Results:** EC002 shows an unbrecciated igneous texture mainly composed of pyroxene and feldspar (~1 mm in size) with scattered prismatic euhedral pyroxene

megacrysts reaching up to 1.5 cm (Fig. 1). A pyroxene megacryst up to 9 cm by 4 cm was reported in [1], but our sample does not contain such giant crystals. The sharp extinction of pyroxene under optical microscope suggests minimal shock metamorphism.

As reported in [1], pyroxene megacrysts show variable chemical compositions, and both orthopyroxene and augite are present (Fig. 1). The most Mg-rich orthopyroxene is  $\text{En}_{85}\text{Wo}_2$ . These xenocrysts are chemically homogeneous at the cores except for the presence of fine exsolution and symplectic inclusions. Some of the augite megacrysts are surrounded with orthopyroxene mantles (~ $\text{En}_{53-56}\text{Wo}_3$ ) and further rimmed by Fe-rich augite (~ $\text{En}_{40-45}\text{Wo}_{30}$ ) at the edges. Fine-grained corona-like features (intergrowth of pyroxene and plagioclase) are observed around some of the orthopyroxene megacrysts.

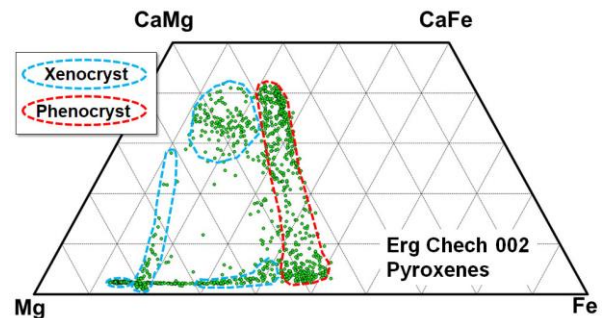


Fig. 2 Pyroxene quadrilateral of EC002, showing diverse xenocryst compositions.

The pyroxenes in the groundmass (areas except for megacrysts) are composite grains of orthopyroxene (~ $\text{En}_{55-45}\text{Wo}_{3.5}$ ) and augite ( $\text{En}_{40-35}\text{Wo}_{40}$ ), each showing fine exsolution lamellae (a few to 10  $\mu\text{m}$  wide). In these pyroxenes, orthopyroxene is located near the center of the grains. The equilibration temperature using these two pyroxene compositions gives *ca.* 800-900  $^{\circ}\text{C}$  [3]. The range is somewhat large due to fine exsolution lamellae which gave overlapping pyroxene compositions even analyzed with FE-EPMA (Fig. 2). The pyroxene grains are prismatic for large grains, but smaller rounded grains are also present.

Feldspar is another major phase in EC002, showing a euhedral to subhedral shape often intergrown with pyroxenes. Feldspar composition is zoned from  $\text{An}_{20}\text{Or}_3$  to  $\text{An}_5\text{Or}_6$  for albitic plagioclase and thin (~10  $\mu\text{m}$  wide) blade-like K-feldspar (~ $\text{An}_4\text{Or}_{65}$ ) exsolution is associated. The Raman analysis of K-feldspar shows

a spectrum similar to that of sanidine rather than orthoclase [4], suggesting formation at high temperature. Similarly, Raman spectra of albite are also similar to those of high-temperature albite rather than Al-Si ordered low-temperature albite. However, the difference is minor and further detailed measurement is required to confirm the feldspar phases.

Minor phases are chromite ( $\text{Cr}_2\text{O}_3=38-49$ ,  $\text{FeO}=35-41$ ,  $\text{TiO}_2=7-15$ , all in wt%), ilmenite, silica, troilite, Ca phosphate and Fe-Ni metal. Opaque minerals show rusting due to terrestrial weathering. Raman analysis of silica minerals shows that most grains are cristobalite, but pseudo-orthorhombic tridymite is also present.

**Discussion and Conclusion:** All the above mineralogy and petrology of our EC002 sample are identical to [1].

Texturally it is likely that pyroxene megacrysts are xenocrysts as their Mg-rich compositions with homogeneous cores is distinct from groundmass phases (Fig. 2). The Fe-Mg compositional gradient of orthopyroxene xenocrysts against the groundmass, now showing the pyroxene overgrowth, can be used to estimate a cooling rate after these megacrysts were incorporated in the groundmass melt and quenched at 800-900 °C, as suggested by pyroxene thermometry. Fig. 3 shows the calculation result of the Fe-Mg zoning profile from the largest orthopyroxene xenocrysts in our PTS. The calculation was performed as a similar manner to [5] employing  $D_{\text{Mg-Fe}}$  in orthopyroxene from [6], assuming that the original composition was homogeneous and modified by atomic diffusion caused by interaction with the surrounding Fe-rich melt. The best fit cooling rate from 1200 °C to 800 °C is about 1 °C/yr. Other orthopyroxene grains also gave similar cooling rates (0.5~2 °C/yr). The obtained fast cooling indicates a quenching episode at high temperature and is consistent with the presence of high-temperature polymorph of feldspar and silica phases as cristobalite and pseudo-orthorhombic tridymite [7].

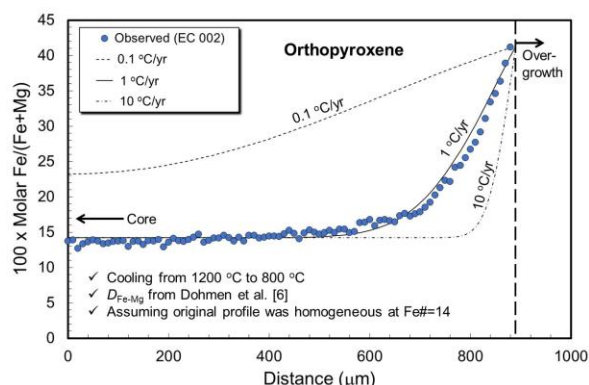


Fig. 3 Calculated cooling rates of the most Mg-rich orthopyroxene xenocryst in EC002 studied.

Since the O-isotope composition of EC002 is intermediate between HEDs and angrites, comparison with these two groups of achondrites is appropriate. As is pointed out in [1], the groundmass texture is similar to equilibrated basaltic eucrites, but feldspar in EC002 is far more Na-K-rich. Also, Fe/Mg-Fe/Mn plots of EC002 pyroxene (both for xenocrysts and phenocrysts) show that they have lower Fe/Mn values compared to those of HEDs and anomalous eucrites although diogenites have some overlapping, suggesting different origins [e.g., 8] (Fig. 4).

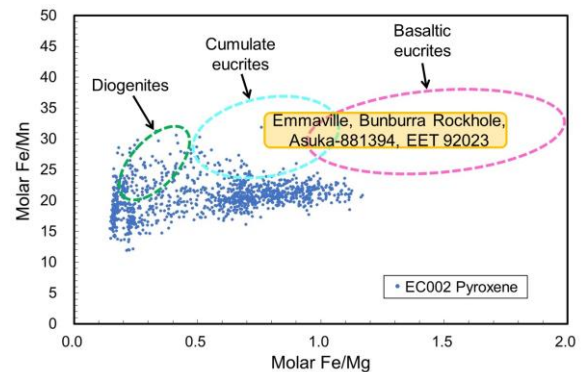


Fig. 4 Pyroxene Fe/Mg versus Fe/Mn diagram. Data for diogenites, eucrites and anomalous eucrites are taken from [8].

It is also unlikely to consider a petrogenetic link to angrites because angrites are highly depleted in alkali elements and different from EC002 [e.g., 9]. However, the presence of megacrystic xenocrysts embedded in the groundmass probably reflects a similar formation process because quenched angrites commonly contain millimeter-sized Mg-rich olivine xenocrysts set in the fine-grained groundmass [e.g., 10]. Although the xenocryst species are different between them (EC002: pyroxene vs. quenched angrites: olivine), an igneous event such as impact melting or endogenous melting to trap deep interior rocks might be common in differentiated bodies in the early solar system.

**References:** [1] <https://www.lpi.usra.edu/meteor/metbull.php?code=72475>. [2] Sanborn M. E. et al. (2019) *GCA*, 245, 577-596. [3] Nakamura Y. et al. (2017) *Meteorit. Planet. Sci.*, 52, 511-521. [4] Freeman J. J. et al. (2008) *Canadian Mineral.*, 46, 1477-1500. [5] Mikouchi T. et al. (2001) *Meteorit. Planet. Sci.*, 36, 531-548. [6] Dohmen R. et al. (2016) *Amer. Mineral.*, 101, 2210-2221. [7] Ono H. et al. (2019) *Meteorit. Planet. Sci.*, 54, 2744-2757. [8] Barrett T. J. et al. (2017) *Meteorit. Planet. Sci.*, 52, 656-668. [9] Mittlefehldt D. W. et al. (2002) *Meteorit. Planet. Sci.*, 37, 345-369. [10] Mikouchi T. et al. (1996) *Proc. NIPR Symp. Antarct. Meteorites*, 9, 174-188.